AD-A107 467 CALIFORNIA UNIV BERKELEY ELECTRONICS RESEARCH LAB F/G 20/9
PLASMA THEORY AND SIMULATION.(U)
JUN 81 C K BIRDSALL N00014-77-C-0578
UNCLASSIFIED NL

END
DATE FILMED
8 81
DTIC

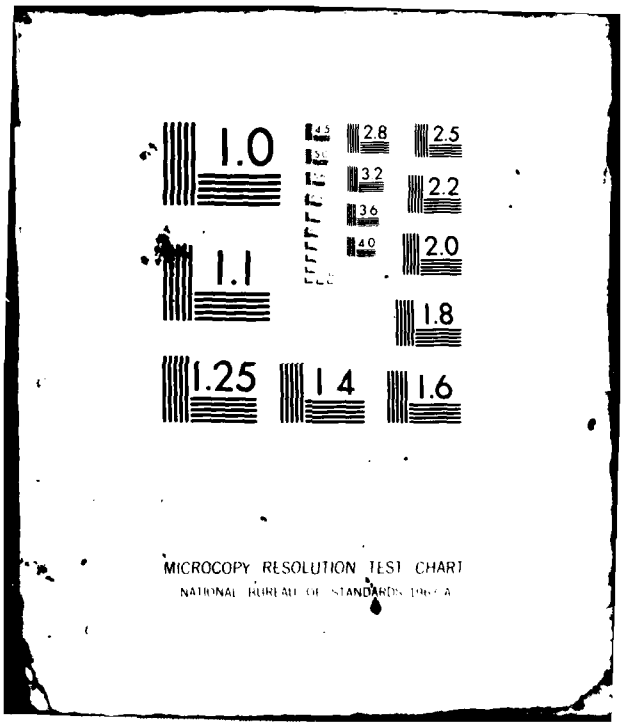
1.0
1.1
1.25
1.4
1.6
1.8
2.0
2.2
2.5
2.8
3.2
3.6
4.0
MICROCOPY RESOLUTION TEST CHART
NATIONAL BUREAU OF STANDARDS 1963 A

Contract N00014-77-C-0578

SECOND QUARTER PROGRESS REPORT
on
PLASMA THEORY AND SIMULATION

April 1 to June 30, 1981

Our research group uses both theory and simulation as tools in order to increase the understanding of instabilities, heating, transport, and other phenomena in plasmas. We also work on the improvement of simulation, both theoretically and practically.

Our staff is —

Professor C.K. Birdsall *Principal Investigator*	191M	Cory Hall	(642-4015)
Dr. Bruce Cohen	L630	LLNL	(422-9823)
Dr. William Nevins *Lecturers, UCB; Physicists LLNL*	L630	LLNL	(422-7032)
Dr. William Fawley	L321	LLNL	(422-9272)
Dr. Alex Friedman	L477	LLNL	(422-0827)
Dr. A. Bruce Langdon *Guests, UCB; Physicists LLNL*	L477	LLNL	(422-5444)
Dr. Mary Hudson *Guest, UCB; Senior Fellow, Space Science Lab.*		SSL	(642-1327)
Mrs. Yu-Jiuan Chen Mr. Douglas Harned Mr. Kwang-Youl Kim Mr. William Lawson Mr. Niels Otani Mr. Stephane Rousset Mr. Vincent Thomas *Research Assistants*	119MD	Cory Hall	(642-1297)
Mr. H. Stephen Au-Yeung *Programmer*	119ME	Cory Hall	(642-3477)
Ms. Ginger Pletcher *Secretary*	119ME	Cory Hall	(642-3477)

June 30, 1981

DOE Contract DE-AT03-76ET53064-DE-AM03-76SF00034
ONR Contract N00014-77-C-0578

ELECTRONICS RESEARCH LABORATORY

University of California
Berkeley, California 94720

TABLE OF CONTENTS

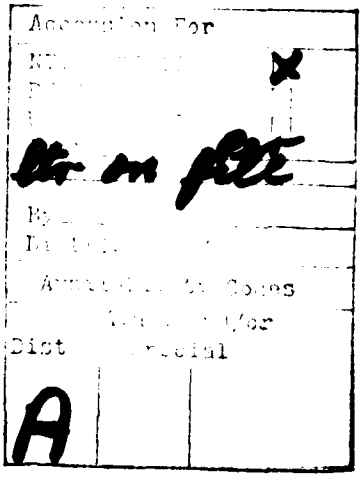

Indicates ONR supported areas

I. PLASMA THEORY AND SIMULATION

A. Lower Hybrid Drift Instability; 2d Simulations and Nonlocal Theory.

Yu-Jiuan Chen (Prof. C.K. Birdsall, W.M. Nevins, LLNL)

This project is now completed. Two ERL reports are being distributed with this QPR. The abstracts are given in Section III-C.

B. Hybrid Simulations of Theta Pinch Rotational Instabilities.

Douglas Harned (Prof. C. K. Birdsall)

This project is now completed. ERL reports are being distributed with this QPR. The abstracts are given in Section III-C.

C. Stability of the Thermal-Barrier Cell of a Tandem Mirror: Electrostatic Simulations

V. Thomas (Prof. C. K. Birdsall)

We are starting to investigate the stability of the thermal-barrier cell of a tandem mirror machine to electrostatic ion-ion two-stream type instabilities using a 1-D electrostatic quasineutral particle simulation code. The code model uses particle ions with two electron components, a "hot" electron component and a "warm" Boltzmann component. The hot electron component is modeled as a fixed negative charge density confined to near the magnetic field minimum. Physically, the hot electrons represent ECRH heated electrons trapped near the minimum in the magnetic field due to their very large magnetic moments. The warm Boltzmann electrons provide charge neutrality. A $-\mu\nabla B$ force is applied to the ions to model the effects of the magnetic well. The field is solved for in this code using

$$ne^{\frac{-q_e\phi}{T_e}} = n_i - n_{f\,fixed}(B) \tag{1}$$

Here $ne^{\frac{-q_e\phi}{T_e}}$ represents the warm Boltzmann electrons and $n_{f\,fixed}(B)$ represents the hot electron component. The quantity n_i is accumulated from the particle ions.

In order to achieve a self-consistent initialization for the code we are required to solve

$$ne^{\frac{-q_e\phi}{T_e}} = e^{\frac{-q_i\phi}{T_i}} \int n_i(v_z,\mu,\phi,B)\,d\mu\,dv_z - n_{f\,fixed}(B) \tag{2}$$

for ϕ as a function of z, the coordinate along the field line. Then, using this self-consistent potential, it is possible to assign appropriate μ and v_z values to the ions.

The choice assumed for the ion distribution function is very important for obtaining well behaved self-consistent potentials*. Some distribution functions give multi-valued potentials near the mirror throat and other distribution functions generate potentials having sheaths, that is locations where the potential has a discontinuity.

We are using a distribution function given in the aforementioned reference which is based upon Fokker-Planck studies of the thermal-barrier cells. The distribution function for ions trapped in the magnetic and electrostatic well of the thermal-barrier cell is taken to be

*Cohen, R. H., "Axial Potential Profiles in Thermal-Barrier Cells," *Nuclear Fusion* 21, 289, February 1981

$$f_t = C\exp^{\frac{E-a\mu B_{max}}{(a-1)T_i}} \tag{3}$$

and the distribution function for the passing ions is given in

$$f_p = C\exp\left[-\frac{E}{T_i}\right] \tag{4}$$

Here C is a normalization constant, E is the energy of the ion, μ is the magnetic moment of the ion (which is treated as an invariant), and B_{max} is the magnetic field magnitude at the mirror throat. The quantity a is a parameter which determines the relative densities of the trapped and passing particles in the Thermal-Barrier cell. An important feature of this model distribution is that the distribution function is continuous across the separatrix. This leads to self-consistent potentials which are, in general, single valued and which vary continuously from the mirror throat to the interior of the thermal-barrier cell. Distribution functions which are not continuous across the separatrix do not have these characteristics in general. The reader is referred to the reference mentioned previously for more details.

D. Alfvén Ion-Cyclotron Instability: Physical Description

Niels F. Otani

The Alfvén ion-cyclotron instability (AIC) is a velocity-space instability believed to occur in the ring-current region of the Earth's magnetosphere [*Thorne*, 1975] and in certain theta-pinch [*Davidson, Ogden*, 1975] and tandem mirror [*Smith, Nevins*, 1981] fusion plasma experiments. As is generally true for velocity-space instabilities, the source of free energy responsible for driving the instability is quite evident; in this case it is $T_{i\perp} > T_{i\parallel}$. Somewhat uncharacteristic of velocity-space instabilities however is the fact that AIC possesses an instability mechanism describable in simple physical terms. This mechanism was described briefly in *Tajima and Dawson*, [1980] and will be amplified here.

We note that the assumptions made in this description are justified by the consistency of the model. In particular we will be assuming that $T_{i\parallel} = 0$ and that $\omega \approx \omega_{ci}$, in order to simplify the description. We are not claiming by these assumptions that AIC does not occur if these assumptions are violated; in fact, for $T_{i\parallel} > 0$, AIC is strongest when ω is appreciably less than ω_{ci} [*Davidson and Ogden*, 1976]. It will be clear however that the essence of the mechanism to be described holds for AIC in general.

AIC is a left-polarized, electromagnetic mode which typically propagates parallel to an unperturbed magnetic field $\mathbf{B}_0$ which we assume to be static and uniform. We also assume $\omega \approx \omega_{ci}$, so the fields and electron $\mathbf{E}_1 \times \mathbf{B}_0$ drifts (designated $(\mathbf{v}_E)_e$) in Figure 1 are rotating counterclockwise around the axis $\mathbf{B}_0$ with frequency ω_{ci}. Since the local unperturbed ion perpendicular velocity distributions (shown as disks) are also rotating with their natural gyrofrequency ω_{ci}, we may think of Figure 1 as rigidly rotating with frequency ω_{ci}, apart from growth effects due to the instability. Alternatively, we may regard Figure 1 as a view of the physics from the corotating frame; in this frame everything is stationary except that the perturbed quantities exhibit pure growth without relative change in orientation. Note however that, in this view, all quantities in Figure 1 continue to be lab frame quantities. We further observe that at a fixed time t, a translation of $\lambda/4$ in the direction of propagation produces a simple clockwise rotation by $\pi/2$ of the physical picture.

With this in mind, start with the perturbed magnetic field $\mathbf{B}_1$ which, as shown at $z = 0$ in Figure 1, is finite since this is an electromagnetic mode and perpendicular to $\mathbf{B}_0$ since $\mathbf{k} \cdot \mathbf{B}_1 = 0$. The quantity $\partial \mathbf{B}_1/\partial t$ has components both along $\mathbf{B}_1$ and perpendicular to $\mathbf{B}_1$ pointing in the direction of rotation, due to the growth rate γ and the rigid rotation $\omega \approx \omega_{ci}$, respectively. Faraday's law dictates that the wave electric field $\mathbf{E}_1$ must encircle $\partial \mathbf{B}_1/\partial t$; this explains the orientation of $\mathbf{E}_1$ at $z = \pm\lambda/4$ in Figure 1.

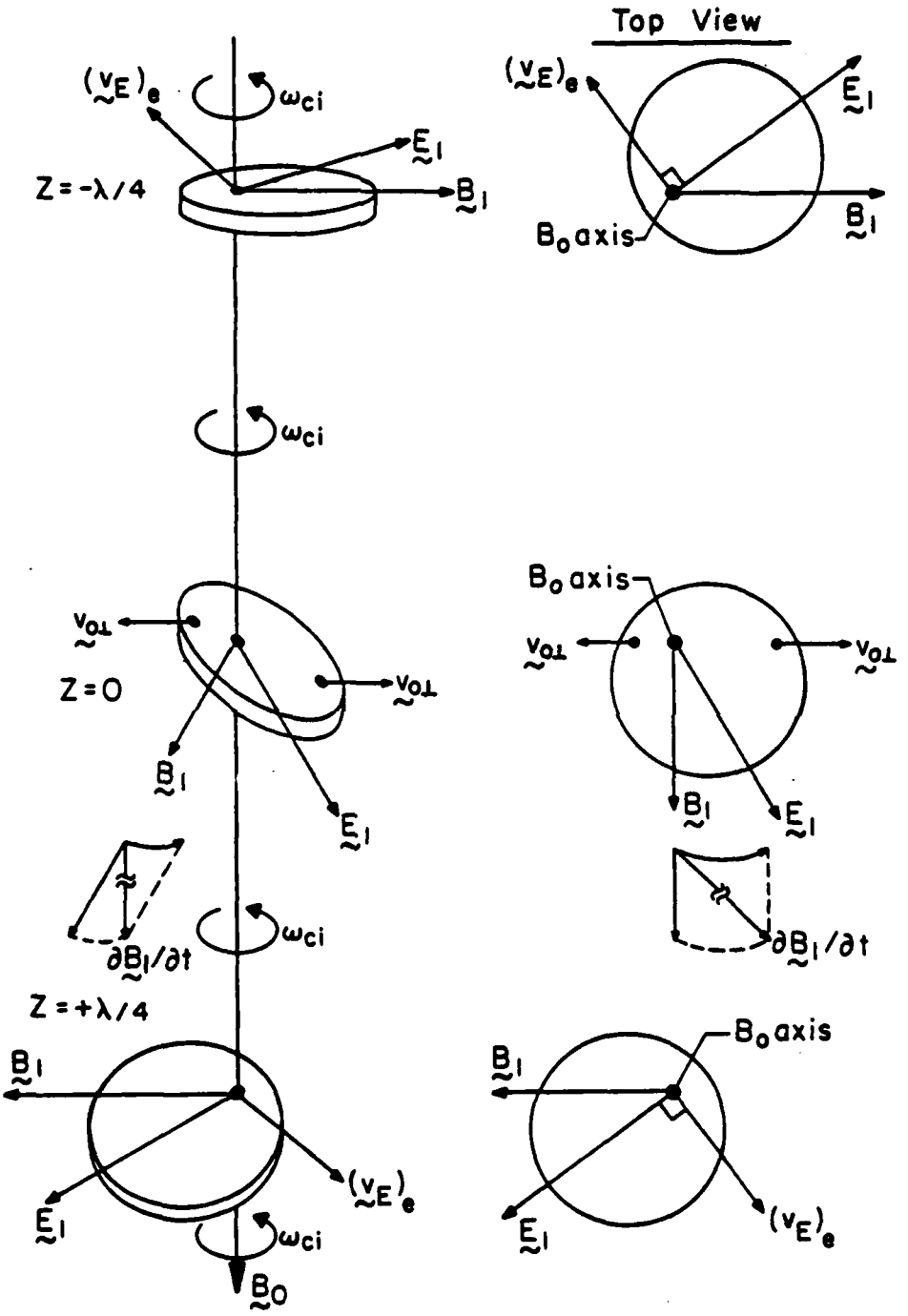
Top View
$(v_E)_e$
ω_{ci}
E_1
B_1
$Z = -\lambda/4$
B_0 axis
$v_{o\perp}$
$Z = 0$
$\partial B_1/\partial t$
$Z = +\lambda/4$
B_0

Figure 1.

This electric field at $z = \pm\lambda/4$ produces two contributions to the perturbed current. First, the electrons drift with velocity $(\mathbf{v}_E)_e = c\mathbf{E}_1 \times \mathbf{B}_0 / B_0^2$ in the direction perpendicular to both $\mathbf{E}_1$ and $\mathbf{B}_0$, assuming negligible electron mass. Second, in the corotating frame of a given ion, the centrifugal force cancels the Lorentz force and the ion is simply accelerated in the direction of the statically oriented electric field. This is pictorially represented in Figure 1 at $z = \pm\lambda/4$ by the uncentered positions of the velocity disk relative to the axis of rotation $\mathbf{B}_0$.

A third contribution to the current at $z = \pm\lambda/4$ arises from the interaction of $\mathbf{B}_1$ with the velocity distribution represented in Figure 1 at $z = 0$. Ions on the left side of the disk are moving to the left and consequently feel a perturbing Lorentz force $e\mathbf{v}_{0\perp} \times \mathbf{B}_1 / c$ directed antiparallel to $\mathbf{B}_0$. Ions on the right side of the disk similarly feel a force parallel to $\mathbf{B}_0$. Since the orientation of $\mathbf{B}_1$ is fixed relative to the ions instantaneously on the left (due to rigid rotation) they are displaced in the $-\mathbf{B}_0$ direction. Similarly, rightward moving ions are displaced in the $+\mathbf{B}_0$ direction. These displacements are represented in Figure 1 by a tilting of the disk. Thus the leftward moving ions are preferentially moved toward $z = -\lambda/4$, contributing to leftward moving current. We see this contribution to the current tends to reinforce $\mathbf{B}_1$ at $z = 0$. In fact this contribution is the destabilizing factor, since clearly the other contributions represent rightward moving current.

In summary, three contributions to the perturbed current have been described. The effect of two of these contributions, the electron and ion responses to the perturbed electric field, is stabilizing. The third contribution, resulting from the selective transport of ions with different perpendicular velocities up and down the zero-order magnetic field, is destabilizing in that it tends to augment the perturbing magnetic field which caused it.

References

Davidson, R. C., and Ogden, J. M. "Electromagnetic Ion Cyclotron Instability Driven by Ion Energy Anisotropy in High-Beta Plasmas," *Phys. Fluids* **18**, 1045, 1975.

Smith, G. R. and Nevins, W. M. "Warm-Ion Stabilization of Alfvén-Ion-Cyclotron Instability," *Mirror Theory Monthly*, Lawrence Livermore National Laboratory, Feb. 15, 1981.

Tajima, T., and Dawson, J. M. "Ion Cyclotron Resonance Heating and the Alfvén-Ion Cyclotron Instability." *Nuclear Fusion* **20**, 1129, 1980.

Thorne, R. M. "Wave-Particle Interactions in the Magnetosphere and Ionosphere." *Rev. Geophys. Space Phys.* **13**, No. 1 291, 1975.

E. Relativistic Quantum Formulation of the Boltzmann Collision Integral

Kwang-Youl Kim (Professor C. K. Birdsall)

The relativistic quantum conductivity tensor for the relativistic plasma is derived by using the relativistic Liouville equation. The quantum relativistic collision integral due to scattering via covariant photons is derived by using relativistic dielectric response function. Our Boltzmann collision integral includes both the collective fluctuation effect and the discreteness of particles on the same footing. The corresponding classical results are obtained by taking the appropriate limits.

II. CODE DEVELOPMENT AND MAINTENANCE

A. Implicit Particle Simulation Using Moments with Orbit Averaging

V. Thomas (B. I. Cohen, Prof. C. K. Birdsall)

The project is now completed. A report has been written (at LLNL). See Section III-D.

B. Plasma Sheath Simulation in 1d

S. Rousset (Prof. C. K. Birdsall)

The numerical model described in the previous Quarterly Progress Report has been implemented. We find that the simulated behaviour of the sheath agrees in some respects with well-known phenomena as predicted by theory.

A new subroutine (called ENTER) has been added, which provides for the simulation of an incoming emitter current. In its present version, this routine adds constant numbers of particles at each time step (there can be one such constant number per species). The particles enter the system at $x=0$; note that we also tried to let new particles enter the sheath at several different positions, but this did not seem to yield any measurable improvement. The initial velocities of the entering particles were chosen (almost) randomly, so that our results had very high noise levels; this last point is still being worked upon.

Since we have new particles entering the system at each time step, and since some arrays in the code have sizes proportional to the total number of simulated particles, we had to deal with the problem of defining the sizes of the arrays in a way such that we never attempt to load particles beyond the limits of these arrays. On the one hand, a straightforward solution is to repack the arrays from time to time, and to expand them whenever we try to go above their upper bounds. On the other hand, we could declare the sizes of the arrays to be much larger than the initial number of particles, adding new particles at the end of the area (of the array) already occupied by other particles. The first solution is very costly, and the second one sets a very stringent limit on the number of time steps in one run. We chose the following compromise: the size of the arrays are chosen equal to the maximum number of particles that will ever be simultaneously in the system; the arrays are repacked at each time step. This very last point means that we could not keep the vectorized option in subroutine MOVE, but we believe that our solution is most efficient in terms of total bank time.

A few other technical features have been implemented: the plots do not include the inverted part of the sheath any more; a call to the PRIOR subroutine has been added, thus allowing the priority to be set automatically at run time.

As a consequence of the modifications described above and in the previous QPR, several new parameters can now be given in the input file:

Name	Function	Default
	For the whole system	
hiprio	Maximum bid priority allowed for the job	1.0
l	Physical length of the system (excluding inverted sheath)	π
ng	Number of spatial cells in the true sheath only	16
nprio	If *nprio*=0, then disable the PRIOR routine	0
nrank	Position of the job in the priority queue	20
phi0	Amplitude of the externally applied potential	0.0
	For each species	
n	Number of particles loaded at time zero	64
nenter	Number of new particles loaded at each time step	1
nmax	Maximum number of particles simultaneously in the system	64

We found the new version of the code to reproduce some of the physical behaviours predicted for a sheath. In particular, some features of Child's law have been successfully

checked for three regimes: without space charge; with space charge and without initial velocity for particles at the emitter; and with space charge and with initial velocity.

References

R. K. Franklin, "Plasma Phenomena in Gas Discharges," Clarendon Press, 1976.

J. K. Boyd, "PRIOR, a Subroutine to Efficiently Set the Running Priority on the Cray Computer," Memorandum number *MFE/CP/80-2432t, 1980.*

C. Quiet-Start Method Comparisons: Random, Bit-Reversed, and Fibonacci Numbers

Yu-Jiuan Chen, and H. Stephen Au-Yeung
(Prof. C. K. Birdsall; Dr. A. B. Langdon, LLNL)

In QPR IV, 1980, we showed that the Fibonacci number and the bit-reversed methods produce very good uniformity and that the random number generator produces considerable local bunching. As a further test, we have also used the cumulative velocity distribution function to assign velocities v_x to a set of beams whose envelope is $f(v_x)$ (as in ES1) and then used the three different number sets to scramble the particle positions, x, to reduce correlations.

For a given non-drifting Maxwellian velocity distribution function, $f(v_x) \sim e^{-v_x^2/2v_t^2}$, the "goodness" of the local thermal equilibria was examined, by calculating the average of the first three velocity moments over various widths $\delta x < L$ (L is the system length and v_t is the thermal speed of this velocity distribution function). By varying the particle number N, we then compared the width δx at which the calculated average local velocity moments departed by 10% from the expected values, for each of the three different number sets, as shown in Figure 1. Note that the expected odd velocity moments vanish for a non-drifting Maxwellian velocity distribution. Therefore, δx's were measured at which the average local odd velocity moments were 10% of v_t^m, where $m = 1$ in Figure 1(a) and 3 in Figure 1(c), respectively. We found that for a large particle number N ($\gtrsim 10^3$) both the Fibonacci number method and bit-reversed method produce very good local thermal equilibria.

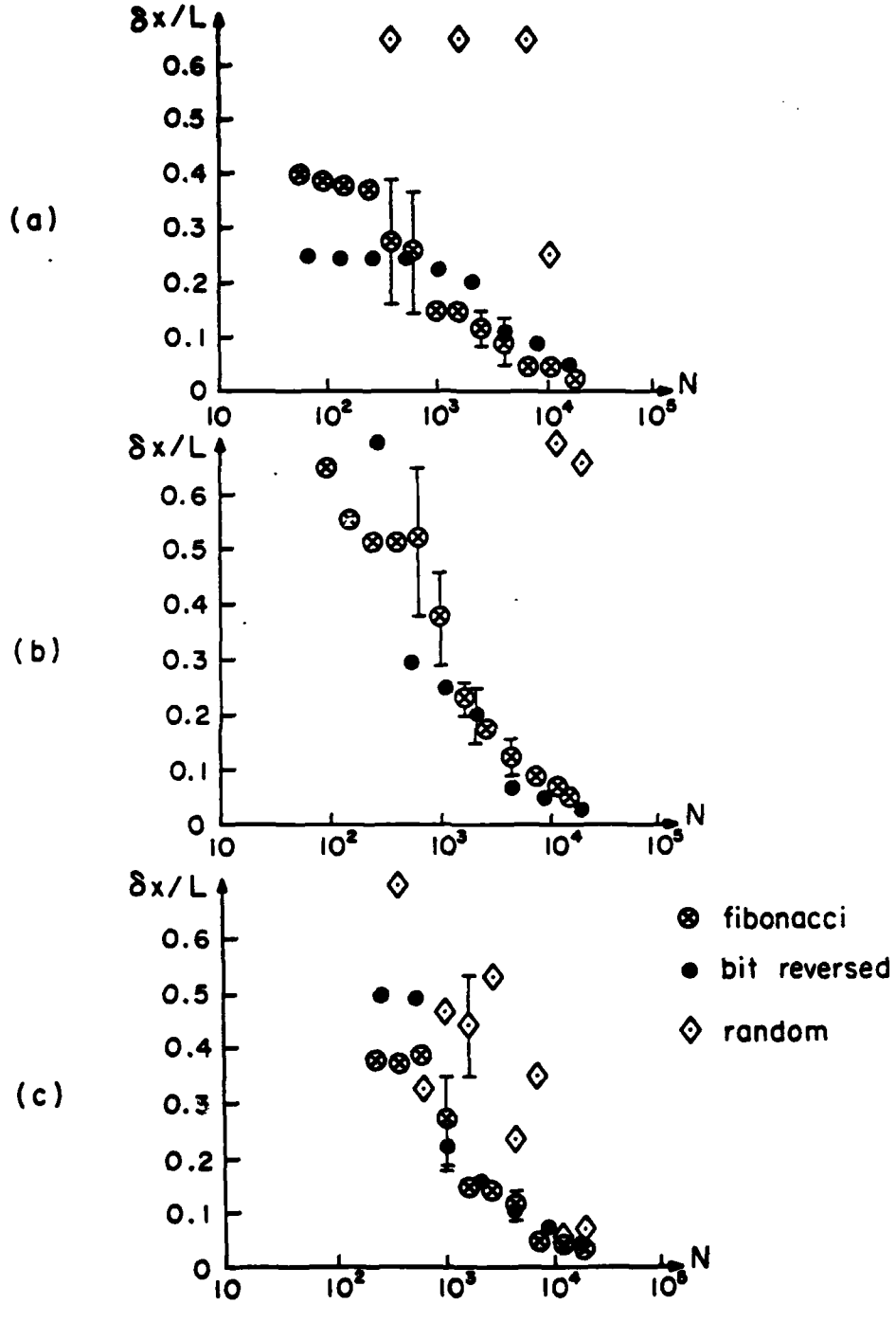

Figure 1. Goodness of the local thermal equilibrium velocity moments as a function of the number of simulation particles used, N. For random, bit-reversed and Fibonacci methods, δx were measured at which (a) $< v >_{\delta x} / v_t = 10\%$ (b) $(< v^2 >_{\delta x} - v_t^2) / v_t^2 = 10\%$ and (c) $< v^3 >_{\delta x} / v_t^3 = 10\%$. Here $< v^m >_{\delta x}$ is the calculated average m^{th} velocity moment over width δx.

III. SUMMARY OF REPORTS, TALKS, PUBLICATIONS, VISITORS

A.

Journal publication: (Completed while Friedman was here; distributed with last QPR)
A. Friedman, R.N. Sudan, and J. Denavit, "A Linearized 3D Hybrid Code for Stability Studies of Field-Reversed Ion Ring," *J. Comput. Phys.* **40**, 1-35, March 1981.

Reprinted from JOURNAL OF COMPUTATIONAL PHYSICS
Vol. 40, No. 1, March 1981
Printed in Belgium

A Linearized 3D Hybrid Code for Stability Studies of Field-Reversed Ion Rings

A. FRIEDMAN* AND R. N. SUDAN

Laboratory of Plasma Studies, Cornell University, Ithaca, New York 14853

AND

J. DENAVIT

Department of Mechanical Engineering and Astronautical Sciences, Northwestern University, Evanston, Illinois 60201

Received May 22, 1979; revised February 7, 1980

A linearized 3D hybrid code, RINGHYBRID, for the study of the low-frequency stability of high-beta equilibria is described. In particular, this code is suitable for application to field-reversed ion rings and mirror plasmas. The code models the development in time of perturbations having a specified azimuthal mode number, l, about an axisymmetric equilibrium state. The equilibrium current is purely azimuthal and is carried entirely by the energetic ion component, which is modeled by discrete simulation particles. This current is consistent with the equilibrium magnetic field and hot-component charge density. In addition to the hot-ion component, a cold uniform density background of ions and a complement of massless electrons are described by fluid equations which incorporate a scalar resistivity. Also presented are verifications of code performance, including tests of cold-plasma normal modes and of plasma return currents arising in response to an azimuthal "drive" current rising linearly with time.

I. INTRODUCTION

In recent years there has been a rebirth of interest in field-reversed configurations, which have the advantage of possessing a region of closed lines for high β plasma confinement surrounded by a region of open lines. This topology requires a relatively simple design for the external magnetic field coils that leads to a major simplification in fusion reactor design. The region of closed lines is produced by internal currents in the plasma. When such currents are force-free the device is known as a spheromak [1]. If the plasma currents flow in the azimuthal direction, only poloidal fields are present and we have a reversed field θ-pinch [2]. A reversed-field mirror [3] is a configuration similar to the θ-pinch except for a lack of axisymmetry introduced by having minimum B quadrupole type coils to provide the external field. The build-up

* Present address: Lawrence Livermore National Laboratory, Livermore, Calif. 94550.

Journal publication: Y-J Chen and B.I. Cohen, "Nonlinear frequency shift induced by the lower-hybrid drift instability," Phys. Fluids 24, 887-892, May 1981.

Nonlinear frequency shift induced by the lower-hybrid drift instability

Yu-Jiuan Chen

Electronics Research Laboratory, University of California, Berkeley, California 94720

Bruce I. Cohen

Lawrence Livermore Laboratory, University of California, Livermore, California 94550
(Received 3 June 1980; accepted 12 February 1981)

It is found that a finite perturbation of the ion orbits leads to a nonlinear frequency shift that reduces the mode frequency and has a weak stabilizing effect on the lower-hybrid drift instability. This result is obtained from a self-consistent solution of the Vlasov–Poisson equations using perturbation theory in which the nonlinear dielectric function and the nonlinear temporal evolution of a single unstable mode in the low drift velocity regime are calculated analytically. The nonlinear frequency shift does not seem to be a potent saturation mechanism in a collisionless plasma, but may be more relevant when there are ion-ion collisions.

I. INTRODUCTION

The linear theory of the lower-hybrid drift instability is well understood and has been discussed in detail by Davidson *et al.*[1] When the amplitude of the wave is small but finite after a time equal to many multiples of the growth time, further evolution will be different from exponential growth at very small amplitudes. In order to analyze this, the nonlinear dielectric response function and the nonlinear temporal evolution of a single unstable mode are derived self-consistently by using perturbation theory to solve the Vlasov and Poisson equations. The single-mode approximation is valid for the instability when the plasma parameters are close to those for linear marginal stability. This requires $v_E \ll v_{ti}$ (the low drift velocity regime) for the lower hybrid drift instability, where $v_E = cE/B$ is the equilibrium $\mathbf{E} \times \mathbf{B}$ drift velocity and $v_{ti}^2 = T_i/M$ is the ion thermal speed. M and T_i are the ion mass and temperature, respectively. Similar single mode studies include: modulation of the Langmuir wave due to weak nonlinearity[2,3]; nonlinear evolution of drift-cyclotron and drift-cone instabilities both in theory[4-7] and simulation.[8]

In this paper we demonstrate that a finite amplitude perturbation of the ion orbits develops during growth which leads to a weakly stabilizing nonlinear shift of the lower-hybrid drift mode frequency. The largest shifts in the mode frequency occur for modes with wavelengths much longer than that of the most unstable mode ($k \ll k_m$), at which wavenumbers the lower-hybrid drift instability converts into the drift cyclotron instability. For simplicity, we use a one-dimensional slab configuration shown in Fig. 1; wave propagation is in the x direction; the magnetic field is uniform and in the z direction; the density gradient is in the y direction. The ions are treated as unmagnetized because the wave frequency and growth rate are much greater than the ion cyclotron frequency. The ions are in force balance; that is, the force due to the ion pressure gradient in the y direction cancels that of the equilibrium electric field. The lower-hybrid drift instability is analyzed in the electrostatic limit; electromagnetic effects are assumed to be small.

In Sec. II, the nonlinear dielectric response is calculated by solving the coupled Vlasov–Poisson equations, and a nonlinear dispersion relation is obtained. Section III is devoted to a derivation of the time evolution of the lower-hybrid drift instability. The field energy level at which saturation might occur and the frequency shift due to the finite amplitude of the wave are also determined. Finally, conclusions and a comparative discussion of several saturation mechanisms are given in Sec. IV.

 0031-9171/81/050887-06$00.90

B.

Abstracts follow of papers submitted to APS Division of Plasma Physics meeting, October 12-16, 1981, New York

Nonlocal Properties of the Lower Hybrid Drift Instabilities* YU-JIUAN CHEN, UC Berkeley, W.M. NEVINS LLNL Using Kinetic theory in the low drift velocity regime and considering only electrostatic perturbations in slab geometry, we found that the lower hybrid drift instability is a negative energy wave driven by resonant ions wherever $\mathrm{sgn}(\omega/k_y)=\mathrm{sgn}\ v_{*e}(k_y)$ as predicted by the local theory, which also says that the local growth rate is largest in the region where the relative drift velocity of electrons and ions is largest. In our non-local analysis this region is an energy source for normal modes. The wave energy propagates from this region across the zero order density gradient to regions where the electron drift velocity v_E equals the wave phase velocity (ω/k_y) and is then absorbed by the resonant electrons. As a result, the unstable normal modes are localized between the regions of high relative drift and electron resonance. The existence of propagation along ∇n was observed first in 2-D particle simulations motivating this theory; the two now check very well. These simulations show that the modes saturate due to both ExB trapping and current relaxation. *Research partially supported by ONR Contract #N00014-77-C-0578 (Berkeley), and in part by DOE Contract # W-7405-ENG-48 (Livermore).

Rotational Instabilities in the Field-Reversed Theta Pinch -- Results of Hybrid Simulations , D.S. HARNED, U.C. Berkeley.* A 2d quasineutral hybrid simulation code has been used to study rotational instabilities in the field-reversed theta pinch. Ions are particles so that both the stabilizing effects of finite Larmor radius and the destabilizing effects of resonant ions are included. For the non-reversed case, our results for the $m=2$ instability, where m is the azimuthal mode number, are comparable to previous theory[1,2]. In contrast, for the reversed case, using parameters like those of FRX-B, we have observed instability for $\alpha<1$ ($\alpha\equiv-\Omega_i/(\Omega_e-\Omega_i)$, where Ω_e and Ω_i are the electron and ion rotational frequencies). This new result is consistent with observations in FRX-B. The threshold value has been found to depend critically on the shape of the pressure profile. As the profile becomes more peaked, the threshold decreases. For sufficiently peaked profiles, unstable modes with $m>2$ have been observed. Nonlinearity has been found to reduce the growth rates for the $m=2$ instability at large amplitude.

1. J.P. Freidberg and L.D. Pearlstein, Phys. Fluids **21**, 1207 (1978).
2. C.E. Seyler, Phys. Fluids **22**, 2324 (1979).

* Work supported by ONR Contract No. N00014-77-C0578.

C.

Abstracts follow of recent ERL reports, most intended for submission to journals, as noted; distributed with this QPR. (Parts of Chen and Harned Ph.D. dissertations)

REVIEW OF THE LOWER HYBRID DRIFT INSTABILITY AND ITS SATURATION MECHANISMS

Yu-Jiuan Chen

Electronics Research Laboratory

University of California, Berkeley, CA. 94720

ABSTRACT

A survey is given of previous research on the linear theory of the lower hybrid drift instability (Sec. I). A summary is made of research recently completed as well as research currently in progress on the nonlinear theory and computer simulations of the lower hybrid drift instability (Sec. II).

Memorandum No. UCB/ERL M81/60 20 August 1981

STABILIZATION OF THE LOWER HYBRID DRIFT INSTABILITY BY RESONANT ELECTRONS

Yu-Jiuan Chen

Electronics Research Laboratory

University of California, Berkeley, California 94720

William M. Nevins

Lawrence Livermore National Laboratory

University of California, Livermore, California 94550

Charles K. Birdsall

Electronics Research Laboratory

University of California, Berkeley, California 94720

ABSTRACT

The lower hybrid drift instability was studied with a two dimensional electrostatic simulation code. Simulations showed good agreement of the measured local growth rates and frequencies with the results of local theory during the early stage of wave growth. At later times nonlocal effects become important, and a coherent mode structure develops. This normal mode was observed to propagate up the density gradient.

At zero plasma beta and zero electron temperature, we found that the lower hybrid drift instability is stabilized by the local current relaxation due to both ion quasilinear diffusion and electron $\vec{E}\times\vec{B}$ trapping which causes electron heating to occur.

ERL Memo. No. M81/72 16 September 1981.
Prepared for submittal to Physics of Fluids.

Quasineutral Hybrid Simulation of Macroscopic Plasma Phenomena

Douglas S. Harned

Electronics Research Laboratory

University of California

Berkeley, CA 94720

ABSTRACT

A method for solving the quasineutral hybrid plasma equations in two dimensions is presented, using full ion dynamics and inertialess electrons. The method is extended to allow plasma-vacuum interfaces of arbitrary shape. The algorithm is applied to the study of rotational instabilities in theta pinch Vlasov equilibria.

ERL Memo. No. M81/71 16 September 1981.
Prepared for submittal to Journal of Computational Physics.

Kink Instabilities in Long Ion Layers

Douglas S. Harned

Electronics Research Laboratory

University of California

Berkeley, CA 94720

ABSTRACT

Kink instabilities in long ion layers immersed in a dense background plasma are studied. A numerical extension of the analytic model of Lovelace indicates that these instabilities will occur for values of the self-magnetic field index below those predicted previously. A quasineutral hybrid simulation code has been used to verify these lower thresholds. The simulations also show that the end of exponential growth occurs due to a nonlinear shift in the betatron frequency at large amplitude, producing an increase in layer thickness and a layer which has many non-axis-encircling ions.

ERL Memo. No. M81/73 16 September 1981.
Prepared for submittal to Physics of Fluids.

Rotational Instabilities in the Field-Reversed Theta Pinch: Results of Hybrid Simulations

Douglas S. Harned

Electronics Research Laboratory

University of California

Berkeley, CA 94720

ABSTRACT

Rotational instabilities in rigidly rotating field-reversed theta pinch equilibria are studied using a quasineutral hybrid simulation code. We observe unstable $m=2$ modes at levels of ion rotation below instability thresholds predicted by finite Larmor radius fluid theory. Nonlinear effects are found to reduce the growth rate and lower the real frequency of the $m=2$ mode at large amplitude. Instabilities with $m>2$ have been observed for some strongly reversed cases. It is also found that growth rates for these instabilities can be greatly reduced by increasing the ratio of the plasma radius to the ion Larmor radius.

ERL Memo. No. M81/70. 16 September 1981.
Prepared for submittal to Nuclear Fusion.

D.

Abstract of Report UCRL-86429 at LLNL follows. This was prepared for submission to Journal of Computational Physics (work done at LLNL and here).

B.I. Cohen, R.P. Freis, V. Thomas, "Orbit-Averaged Implicit Particle Codes"

ORBIT-AVERAGED IMPLICIT PARTICLE CODES

Bruce I. Cohen and Robert P. Freis
Lawrence Livermore National Laboratory, University of California
Livermore, California 94550

and

Vincent Thomas
Electronics Research Laboratory, University of California
Berkeley, California 94720

ABSTRACT

This paper reports the merging of orbit-averaged particle code techniques with recently developed implicit methods to perform numerically stable and accurate particle simulations. Implicitness relaxes time-step constraints. Orbit averaging allows one ensemble of particles to represent many ensembles of particles distributed with respect to a phase variable over the phase-space trajectories. In simulation models where the electromagnetic fields are calculated with the time step much longer than the step used for particle pushing, a large reduction in the statistical requirements on particles can result from orbit averaging. Implicitness and orbit averaging can extend the applicability of particle codes to the simulation of long time-scale plasma physics phenomena such as transport and low-frequency instabilities in controlled fusion devices. Difference equations for electrostatic and magneto-inductive physics models are presented, and analyses of the numerical stability of each scheme are given. Simulation examples are presented for a one-dimensional electrostatic model and for a two-dimensional magneto-inductive model.

UCRL - 86429 PREPRINT (LLNL) 29 July 1981

DISTRIBUTION LIST 1

Department of Energy

Manley, Nelson, Sadowsky, Dobrott
Lankford

Department of Navy

Condell, Roberson, Florance

Austin Research Associates

Drummond, Moore

Bell Telephone Laboratories

Hasegawa

Calif. Institute of Technology

Liewer

Calif. State Polytech. Univ.

Rathman

Columbia University

Chu

Cornell University

Mankofsky

Electrical Power Research Inst.

Gough, Scott

General Atomic Company

Helton, Lee

Georgia Institute of Technology

Bateman

Hascom Air Force Base

Rubin

IBM Corporation

Gazdag

JAYCOR

Klein, Tumolillo, Hobbs

Kirtland Air Force Base

Pettus

Los Alamos Scientific Laboratory

Barnes, Burnett, Forslund, Gitomer, Hewett, Lindemuth, Mason, Neilson, Oliphant, Sgro

Lawrence Berkeley Laboratory

Cooper, Kaufman, Kim, Kunkel, Pyle, Sternlieb

Lawrence Livermore National Laboratory

Albritton, Anderson, Brengle, Briggs, Bruijnes, Byers, Chambers, Cohen, Drupke, Estabrook, Fawley, Finan, Fraas, Fuss, Harte, Killeen, Kruer, Langdon, Lasinski, Lee, Maron, Matsuda, Max, McNamara, Mirin, Nevins, Nielson, Smith, Tull

Mass. Institute of Technology

Berman, Bers, Gerver, Kulp, Palevsky

Mission Research Corporation

Godfrey

U. S. Naval Research Laboratory

Boris, Drobot, Craig, Haber, Orens, Vomvoridis, Winsor

Northwestern University

Denavit

New York University

Grad, Weitzner

Oak Ridge National Laboratory

Dory, Meier, Mook

Princeton Plasma Physics Laboratory

Chen, Cheng, Lee, Okuda, Tajima, Tang

Princeton University

Graydon

DISTRIBUTION LIST 2

Science Applications, Inc.

McBride, Siambis, Wagner

Sandia Laboratories, Albuquerque

Freeman, Poukey, Quintenz

Sandia Laboratories, Livermore

Marx

Massachusetts

Johnston

Stanford University

Buneman

University of Arizona

Morse

Univ. of California, Berkeley

Arons, AuYeung, Birdsall, Chen, Chorin, Friedman, Grisham, Harned, Hudson, Keith, Lichtenberg, Lieberman, McKee, Otani, Potter, Thomas

University of California, Davis

DeGroot, Woo

University of California, Irvine

Rynn

University of Calif., Los Angeles

Dawson, Decyk, Huff, Lin

University of Iowa

Joyce, Knorr, Nicholson

University of Maryland

Guillory, Rowland, Winske

University of Pittsburgh

Zabusky

University of Texas

Horton, MacMahon

University of Wisconsin

Shohet

Culham Laboratory

Eastwood,, Roberts

University of Reading

Hockney

Ecole Polytechnique / Centre de Polytech.

Adam

Bhabha Atomic Research Centre

Aiyer, Gioel

Isreal

Gell

Tel-Aviv University

Cuperman

Kyoto University

Abe

Nagoya University

Kamimura

Max Planck Inst. fur Plasmaphysik

Biskamp, Kraft

Universitat Kaiserslautern

Wick

University of Innsbruck

Kuhn

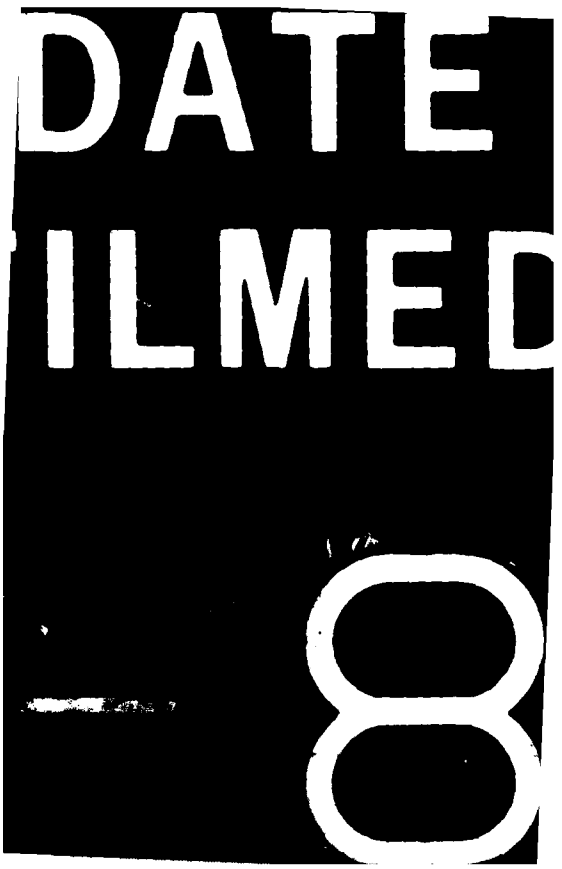
DATE
ILMED
8